Supplementary Materials for

Mixed Conductive Composites for 'Low-Temperature' Thermochemical CO_2 Splitting and Syngas Generation

The PDF file includes:

recently published redox catalysts on methane POx and CO_2 splitting

XRD characterization

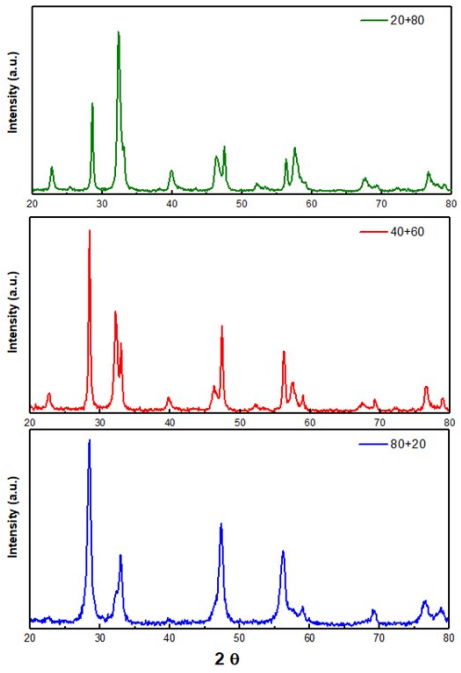

Fig. S1 XRD patterns of CGCO/LNF at different ratios 20/80; 40/60; 80/20.

TPR demonstrated that the weight loss of CGCO, LNF and CGCO/LNF 60/40 during CH_4-TPR and H_2-TPR. It was evident that the weight of LNF in **Fig.S2 (a)** was increased rapidly after 700 ^oC, indicating the pure LNF was prone to coke in the reducing gas of methane. In compare, the weight of CGCO/LNF 60/40 in the methane atmosphere did not show the apparent weight gain until 800 ^oC.

To eliminate the influence of coke, the H_2-TPR experiments were tested to see the weight loss at the temperature range of 100 ^oC to 850 ^oC shown in **Fig. S2(b)**. It was observed that the weight loss of CGCO/LNF 60/40 was almost the same as the LNF. Because the weight loss of standalone CGCO is only 1.5%, about 4% weight loss of CGCO/LNF 60/40 might come from the extra oxygen removal of CGCO and LNF in the mixed conductive composites. It indicated that the synergistic effect of the mixed conductive composites could facilitate 1.4% more oxygen removal from the two oxygen suppliers considering the weight ratio of CGCO and LNF.

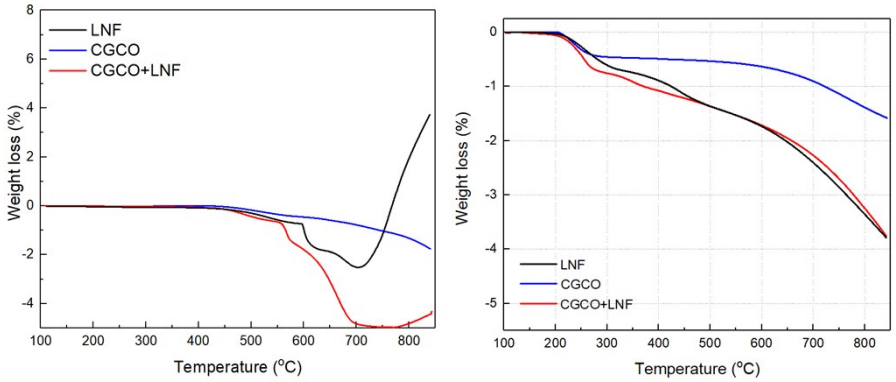

(a) CH_4-TPR (b) H_2-TPR

Fig. S2 Weight loss of mixed conductive composites CGCO/LNF 60/40 in (a) CH_4 TPR and (b) H_2 TPR.

Isothermal Redox cycles

It showed that the mixed conductive material CGCO/LNF exhibited good kinetics with a higher oxygen migration rate both in reduction and oxidation steps. It was observed that both standalone CGCO and LNF exhibited a single lattice oxygen extraction peak within the first half-minute of methane-POx step (**Fig. S3 750ºC**). As a comparison, CGCO/LNF composites exhibited both the lattice oxygen extraction peak at 0.5 min and a "plateau-like" lattice oxygen extraction curve from t = 0.5 min to t = 2.0-4.0 min. This might indicate that the CGCO/LNF composite was "activated" at the beginning of the methane-PO_x step, following with steady lattice oxygen extraction afterward.

The kinetics of Reduction and oxidation

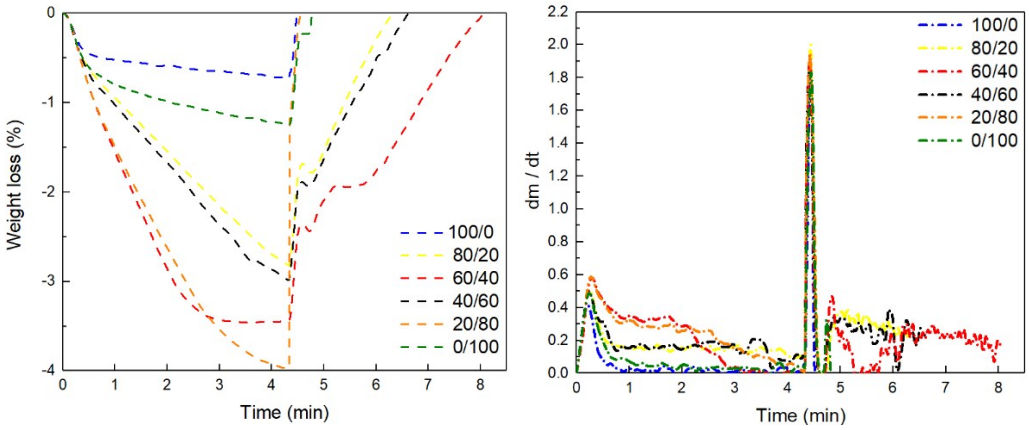

(a)

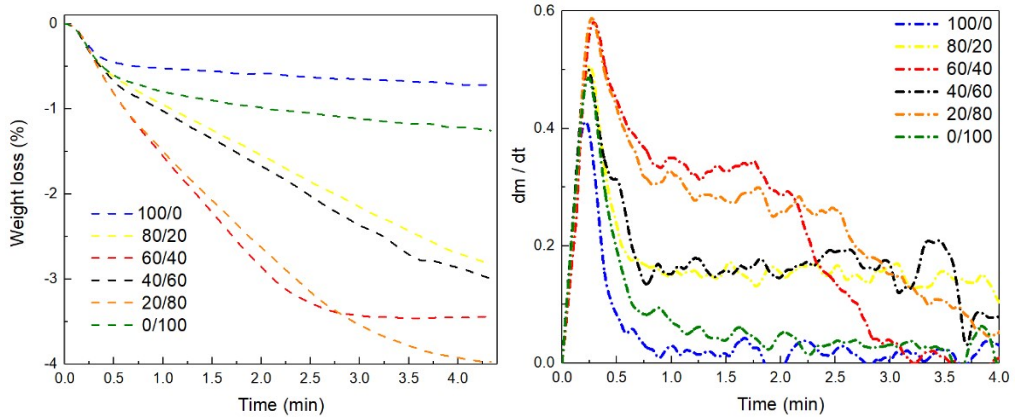
Weight loss (%)
Time (min)
100/0
80/20
60/40
40/60
20/80
0/100
dm / dt
Time (min)
100/0
80/20
60/40
40/60
20/80
0/100

(b)

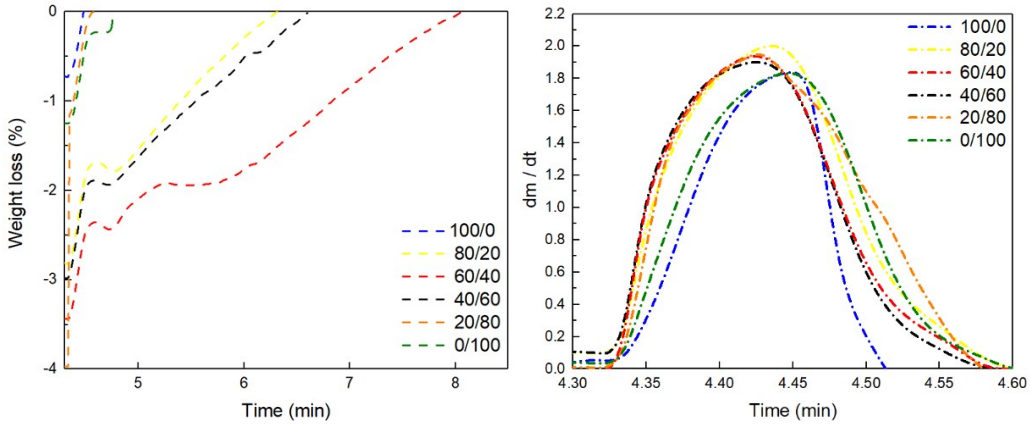
Weight loss (%)
Time (min)
100/0
80/20
60/40
40/60
20/80
0/100
dm / dt
Time (min)
100/0
80/20
60/40
40/60
20/80
0/100

(c)

750°C

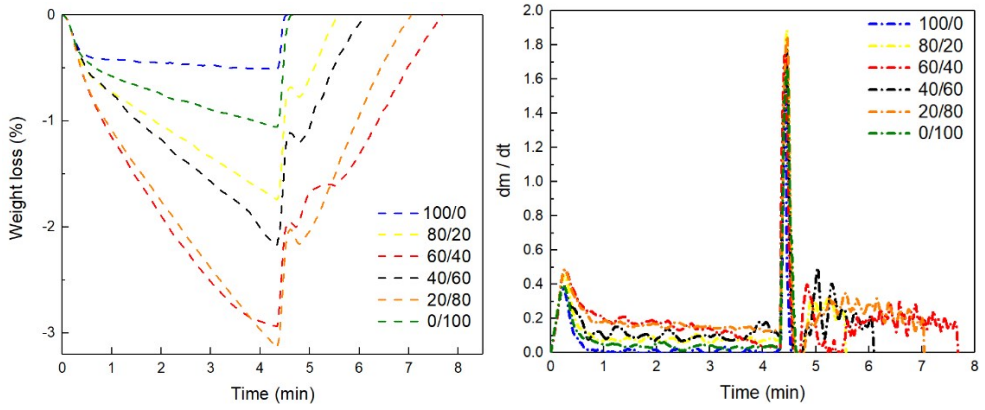
Weight loss (%)
Time (min)
100/0
80/20
60/40
40/60
20/80
0/100
dm / dt
Time (min)
100/0
80/20
60/40
40/60
20/80
0/100

(a)

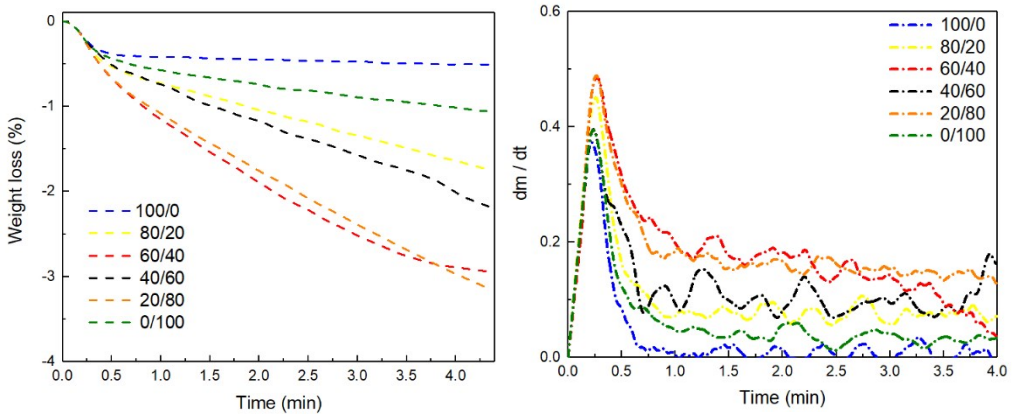
Weight loss (%)
Time (min)
100/0
80/20
60/40
40/60
20/80
0/100
dm / dt
Time (min)
100/0
80/20
60/40
40/60
20/80
0/100

(b)

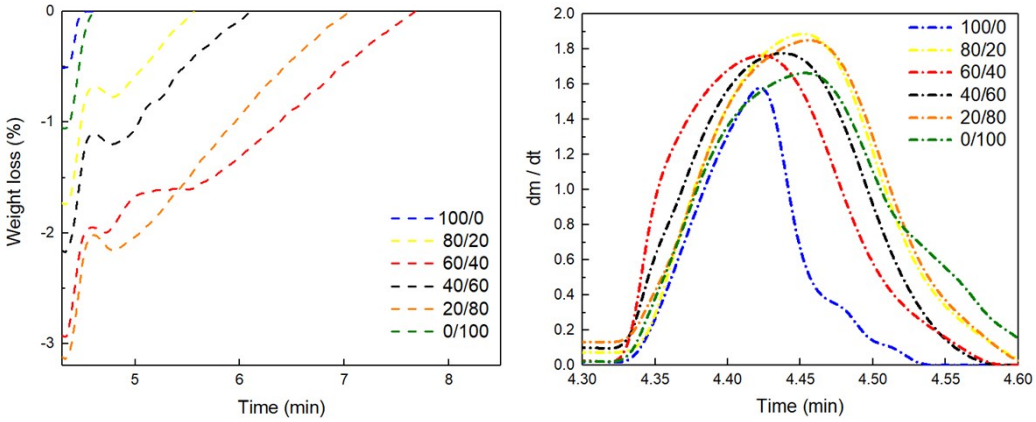
Weight loss (%)
Time (min)
100/0
80/20
60/40
40/60
20/80
0/100
dm / dt
Time (min)
100/0
80/20
60/40
40/60
20/80
0/100

(c)

700°C

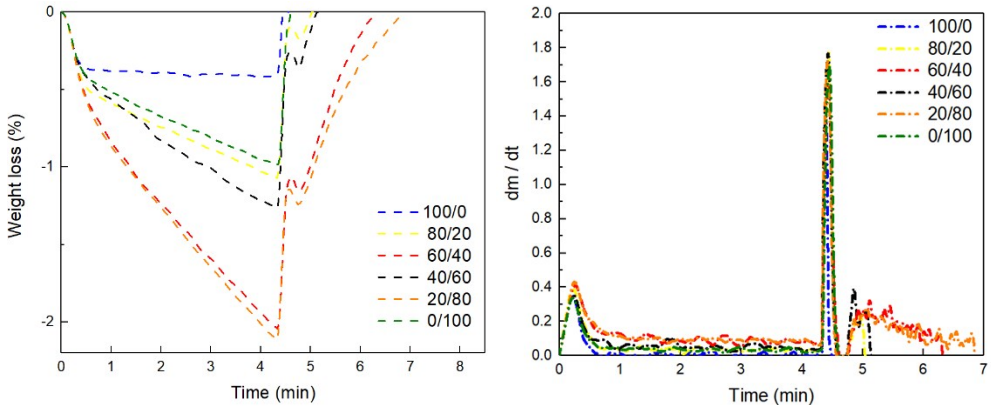
Weight loss (%)
Time (min)
100/0
80/20
60/40
40/60
20/80
0/100
dm / dt
Time (min)
100/0
80/20
60/40
40/60
20/80
0/100

(a)

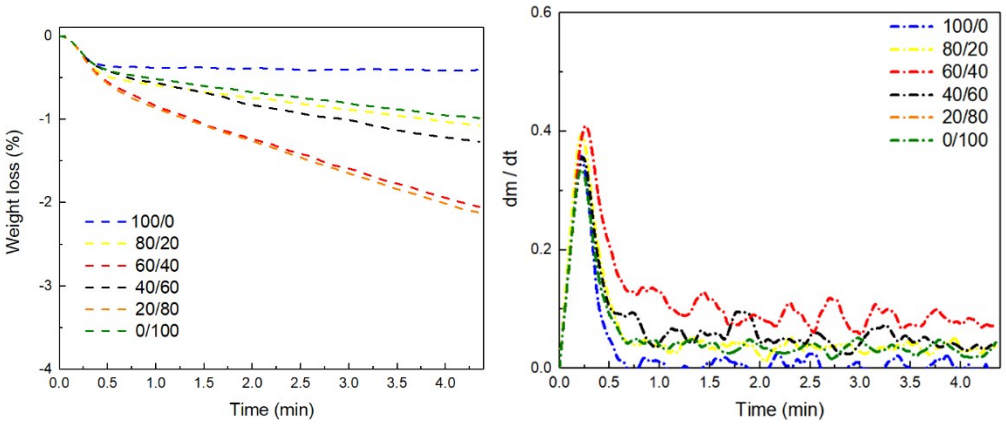
Weight loss (%)
Time (min)
dm / dt
100/0
80/20
60/40
40/60
20/80
0/100

(b)

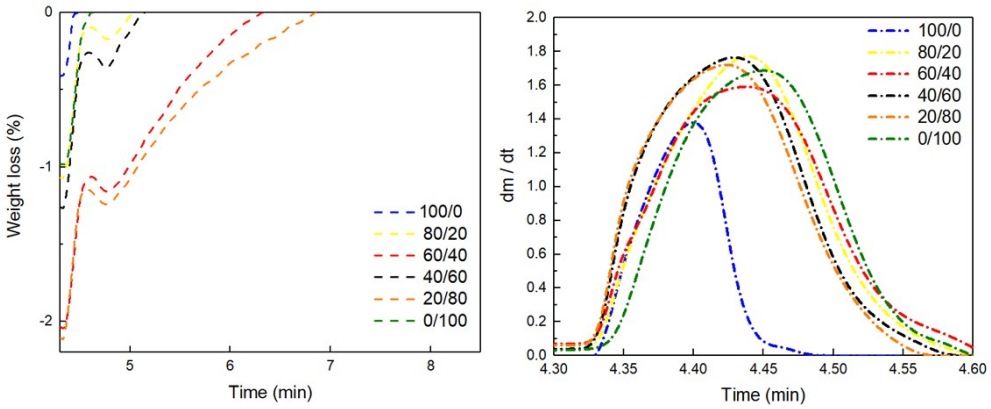
Weight loss (%)
Time (min)
dm / dt
100/0
80/20
60/40
40/60
20/80
0/100

(c)

650°C

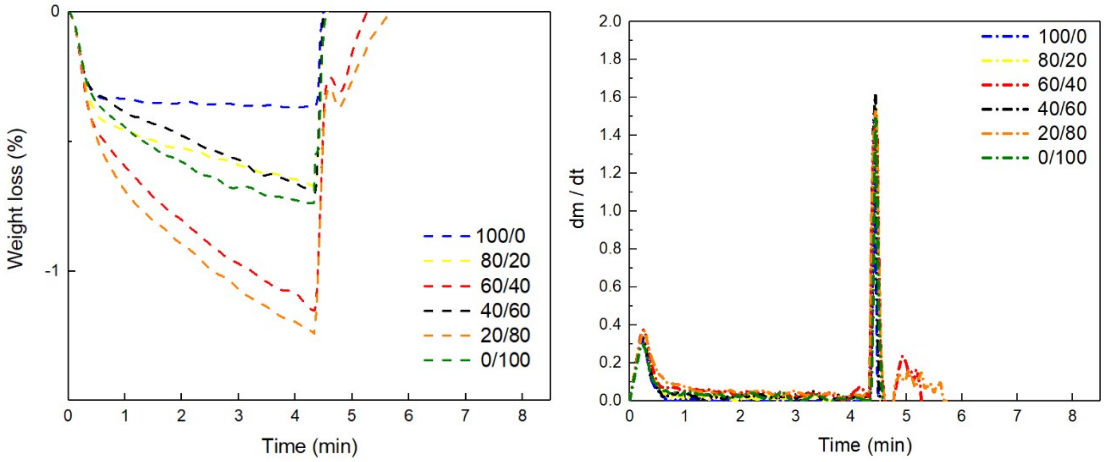
Weight loss (%)
Time (min)
dm / dt
100/0
80/20
60/40
40/60
20/80
0/100

(a)

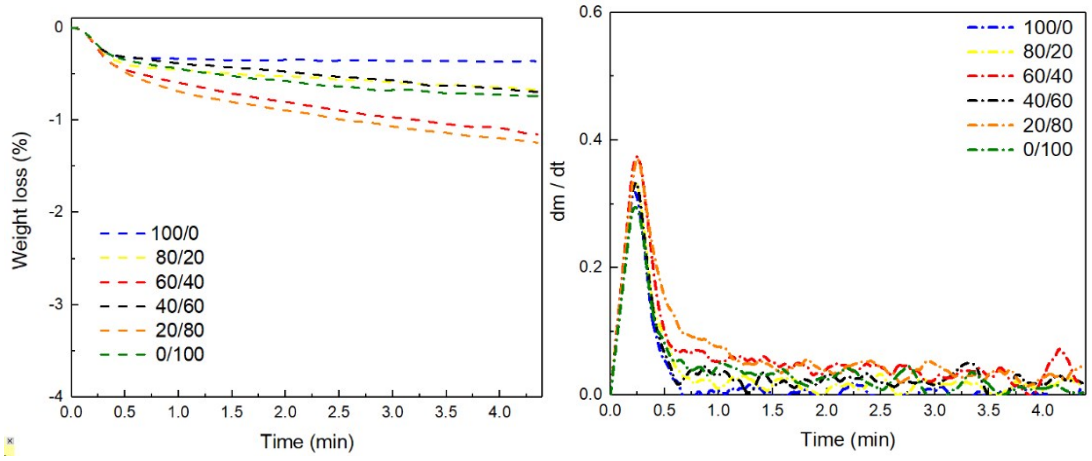

(b)

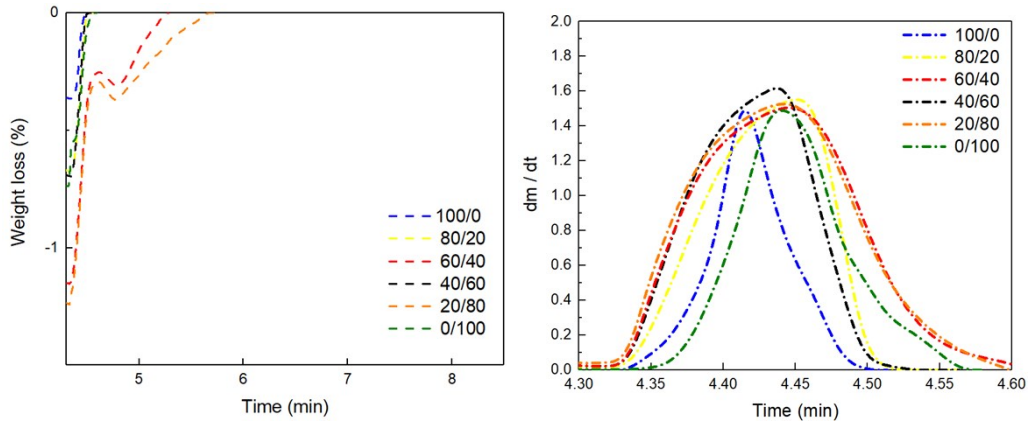

(c)

600ºC

Fig. S3 Kinetics TA- DTG Redox Material mass change in the 5% CH_4/Ar for reduction step for cycled CGCO (100/0), CGCO/LNF (80/20, 60/40, 40/60, 20/80), LNF (0/100), at the temperature of 750ºC, 700 ºC, 650 ºC, 600 ºC. (a) redox cycle and (b) reduction, and (c) oxidation step.

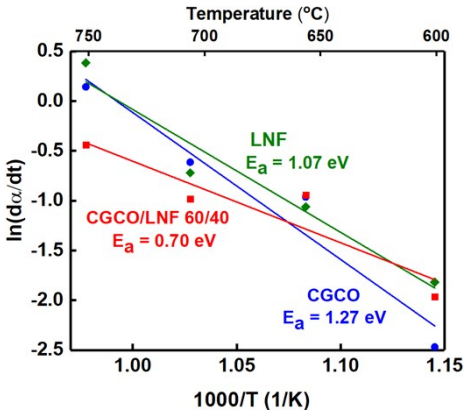

Fig. S4 Apparent activation energies of methane POx for CGCO, LNF, and CGCO/LNF 60/40.

Analysis of the apparent activation energy of the methane POx process.

The methane reduction kinetics of CGCO, LNF and CGCO/LNF 60/40 can be compared in terms of dimensionless conversion (α *vs.* t) and its derivative (dα/dt *vs.* α). A model-free (isoconversional) kinetics method[1] were used on the processed TGA data in order to obtain approximate activation energy and qualitative insights for the reduction of CGCO, LNF and CGCO/LNF 60/40 by methane. According to the equation: $\left[\frac{\partial \ln\left(\frac{d\alpha}{dt}\right)}{\partial T^{-1}}\right]_{\alpha} = -\frac{E_a}{R}$ (α=const), the temperature dependence of the isoconversional reaction rate can be used to evaluate isoconversional values of the activation energy. We determined the activation energies at several fixed conversion numbers between 20% and 50% (the rates at initial and final reaction stages are less reliable). Similar apparent activation energies were obtained at different conversion numbers selected. In **Fig. S4**, we illustrated 40% conversion as the calculation standard, where the activation energy was best approximated by the average value. Finally, the activation energy of methane reduction on standalone CGCO, LNF and the mixed composite CGCO/LNF 60/40 were calculated by the isoconversional method over the temperature range from 600 °C to 750 °C.

Definition of reactivity parameters

The results of partial oxidation of methane and CO_2 splitting at 750 °C are shown in **Fig. 4** by using CH_4 conversion, CO selectivity, CO_2 conversion, and O extracted. For the experiments, the methane and CO_2 conversion are defined as:

$$CH_4\ conversion\ \% = \frac{Moles\ of\ CH_4\ consumed}{Moles\ of\ CH_4\ introduced} * 100\% \quad (1)$$

$$CO_2\ conversion\ \% = \frac{Moles\ of\ CO_2\ consumed}{Moles\ of\ CO_2\ introduced} * 100\% \quad (2)$$

The CO selectivity is defined as:

$$CO\ selectivity\ \% = \frac{Moles\ of\ CO\ produced}{Moles\ of\ CO\ and\ CO_2\ produced} * 100\% \quad (3)$$

The O extracted wt. % is defined as:

$$O\ extracted\ \% = (Moles\ of\ CO\ produced + 4 * Moles\ of\ CO_2\ produced) * 1(\quad (4)$$

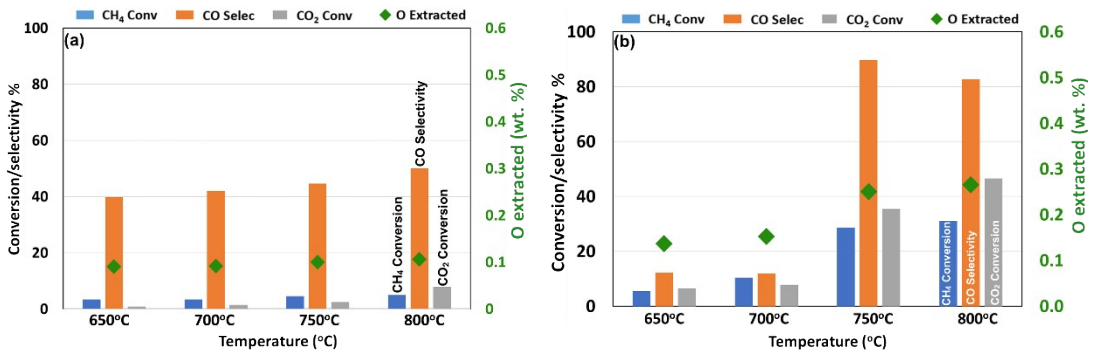

Fig. S5 Effect of temperature on the reactivity of (a) CGCO and (b) LNF.

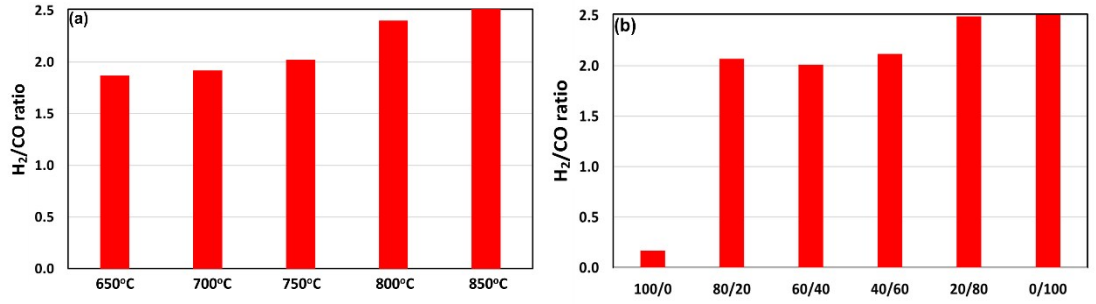

Fig. S6 Effect of (a) temperature and (b) different ratios of CGCO and LNF on the coke formation of CGCO/LNF (H_2/CO ratio).

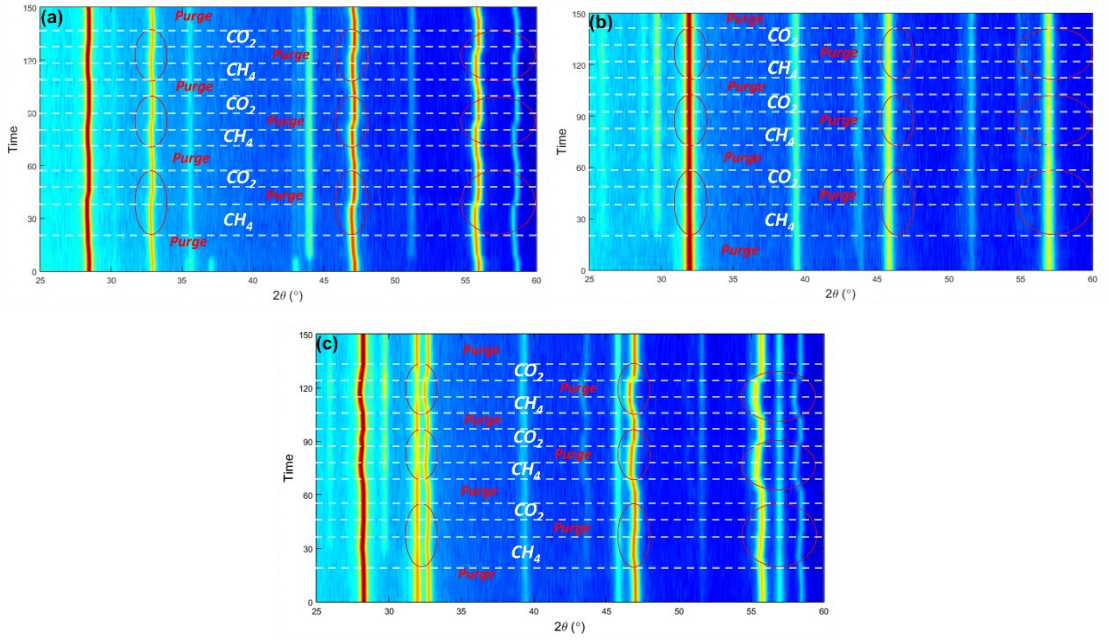

Fig. S7 *In-situ* XRD patterns of (a) CGCO and (b) LNF during the three redox cycles at 750°C; (c) CGCO/LNF 60/40 for three redox cycles.

Table S1. Quantification from Rietveld refinement on standalone CGCO, LNF and CGCO/LNF with CGCO/LNF = 60/40 weight ratio (equal to 67.6/32.4 molar ratio)

	Oxygen extraction from the oxygen recourse			
	Standalone CGCO	**Standalone LNF**	**CGCO in CGCO/LNF**	**LNF in CGCO/LNF**

Rietveld refinement	0.86 wt.%	0.86 wt.%	3.81 wt.%	1.88 wt.%
Experimental (TGA)	0.65 wt.%	1.03 wt.%	NA	NA
	Total oxygen extraction from CGCO/LNF 60/40			
Rietveld refinement	0.68*3.81 wt.% + 0.32*1.88 wt.%		3.18 wt.%	
Experimental (TGA)	NA		3.4 wt.%	

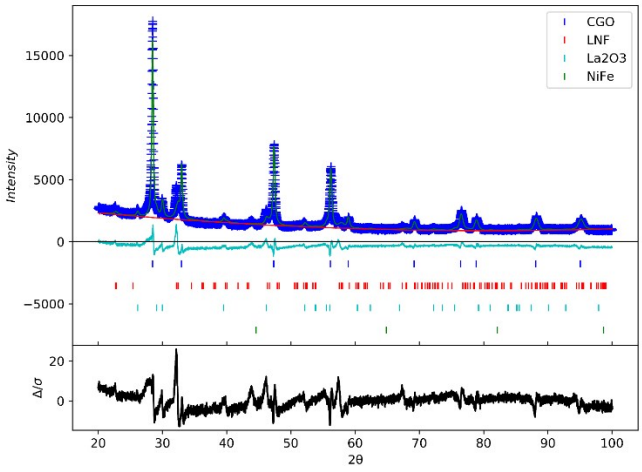

CGCO-LNF reduced

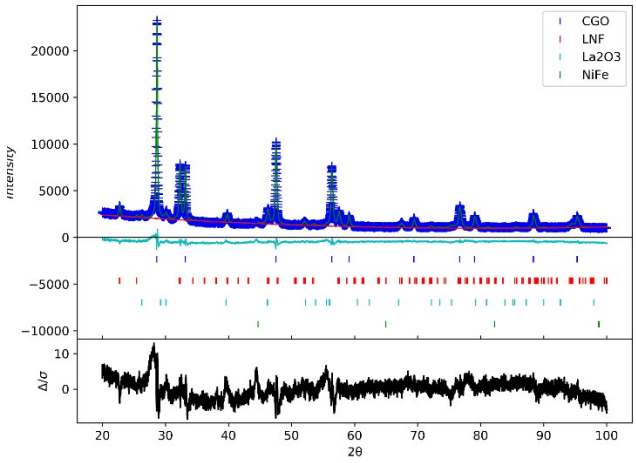

CGCO-LNF oxidized

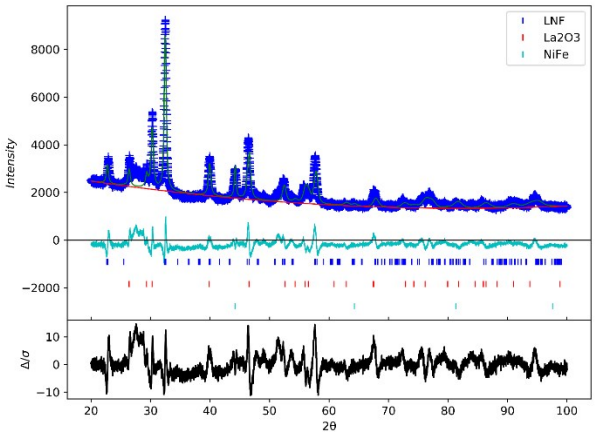

LNF reduced

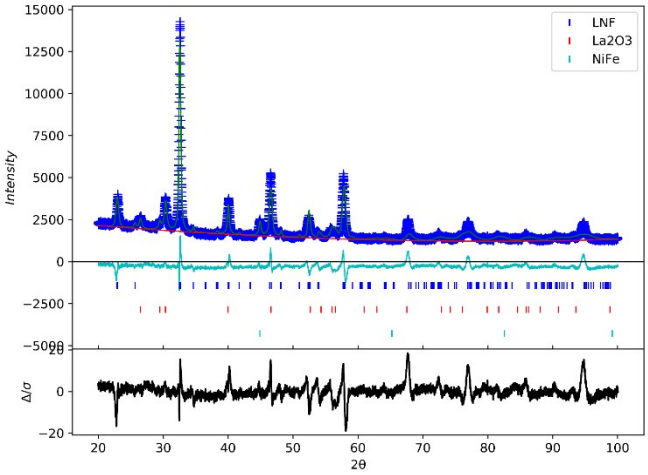

LNF oxidized

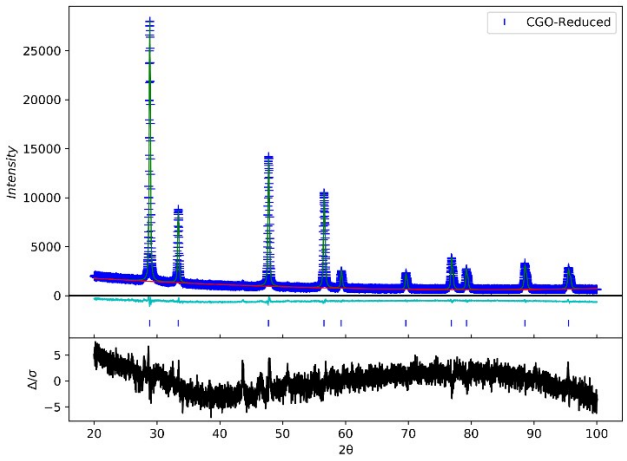

CGCO reduced

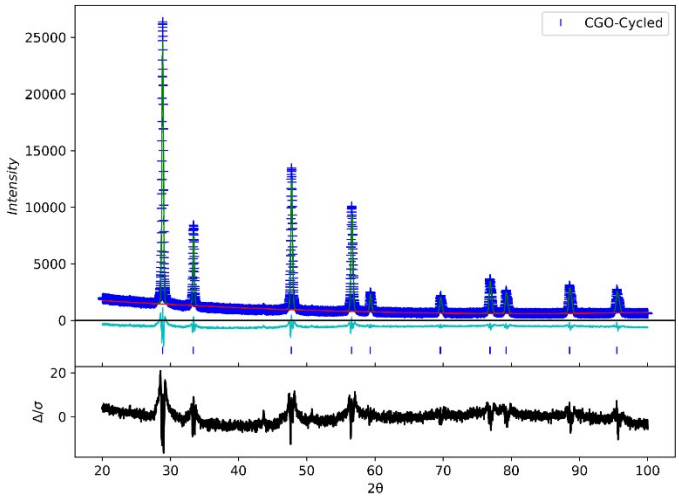

CGCO oxidized

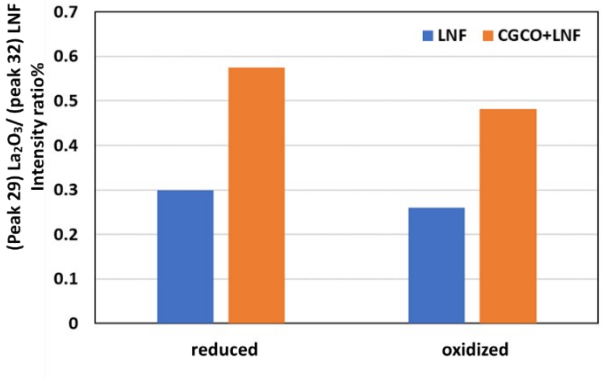

Fig. S8 The intensity ratio of La_2O_3 at peak 29 and LNF at peak 32.

TEM

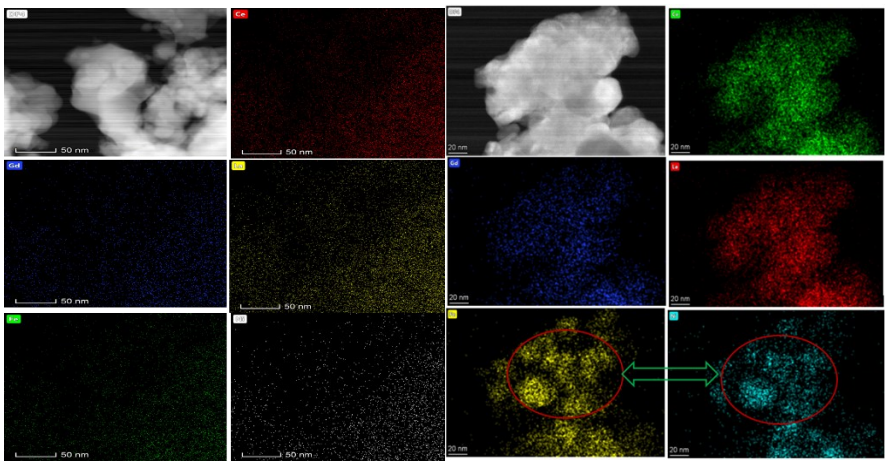

(a) (b)

Fig. S9 The STEM and EDX mappings of (a) fresh and (b) reduced CGCO/LNF 60/40.

SEM

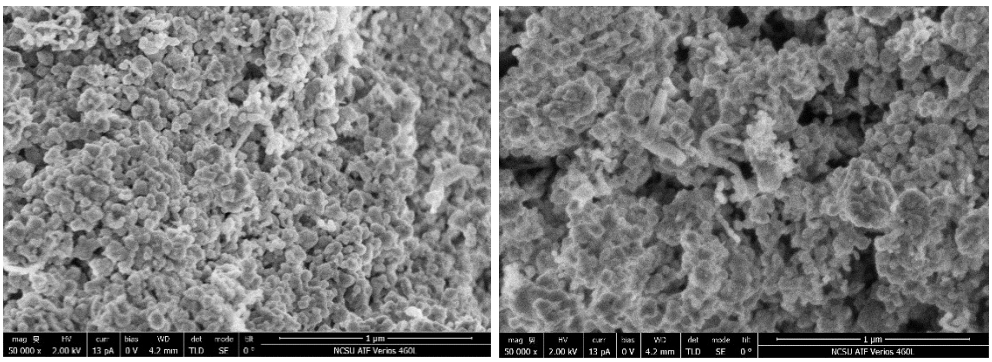

Fig. S10 SEM images of the CGCO/LNF 60/40 fresh and cycled.

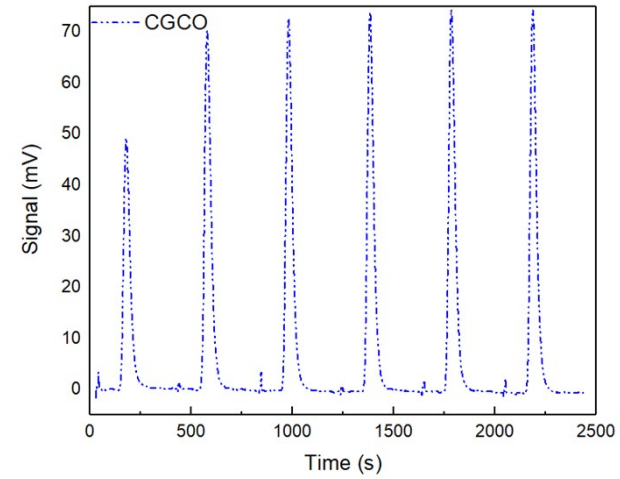

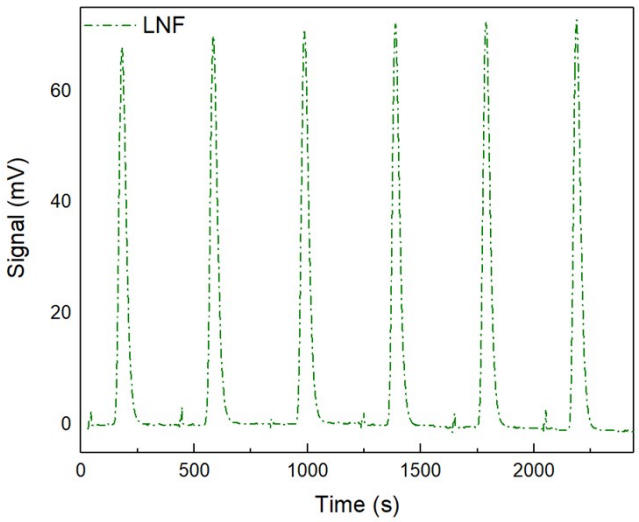

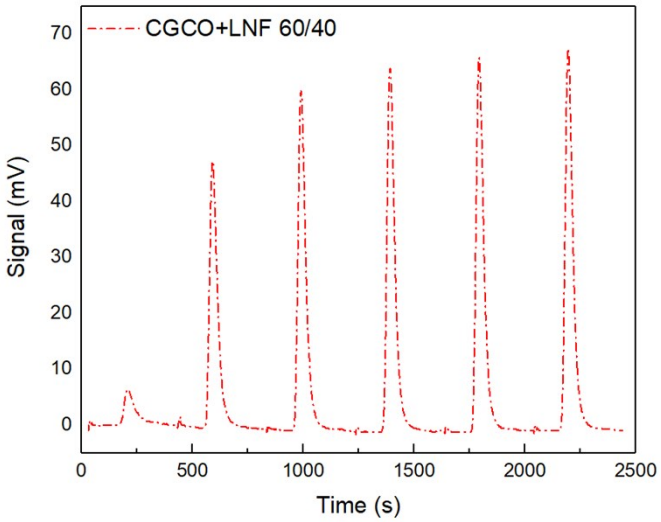

Fig. S11 The absorption signal in six CO pulses.

Table S2. CO chemisorption for CGCO, LNF, CGCO/LNF 60/40 (sample=0.3 g)

	CO adsorption (mol)			Total CO adsorption (mol g^{-1})
	1st pulse	2nd pulse	3rd pulse	
CGCO	9.99×10^{-7}	1.58×10^{-7}	4.52×10^{-8}	4.01×10^{-6}
LNF	2.46×10^{-7}	9.14×10^{-8}	7.10×10^{-9}	1.10×10^{-6}
CGCO/LNF 60/40	2.57×10^{-6}	7.83×10^{-7}	2.65×10^{-7}	1.21×10^{-5}

Table S3. The specific surface areas of CGCO, LNF, and CGCO/LNF 60/40 by BET test

	BET surface area (m^2/g)
CGCO	4.02
LNF	8.35
CGCO/LNF 60/40	17.09

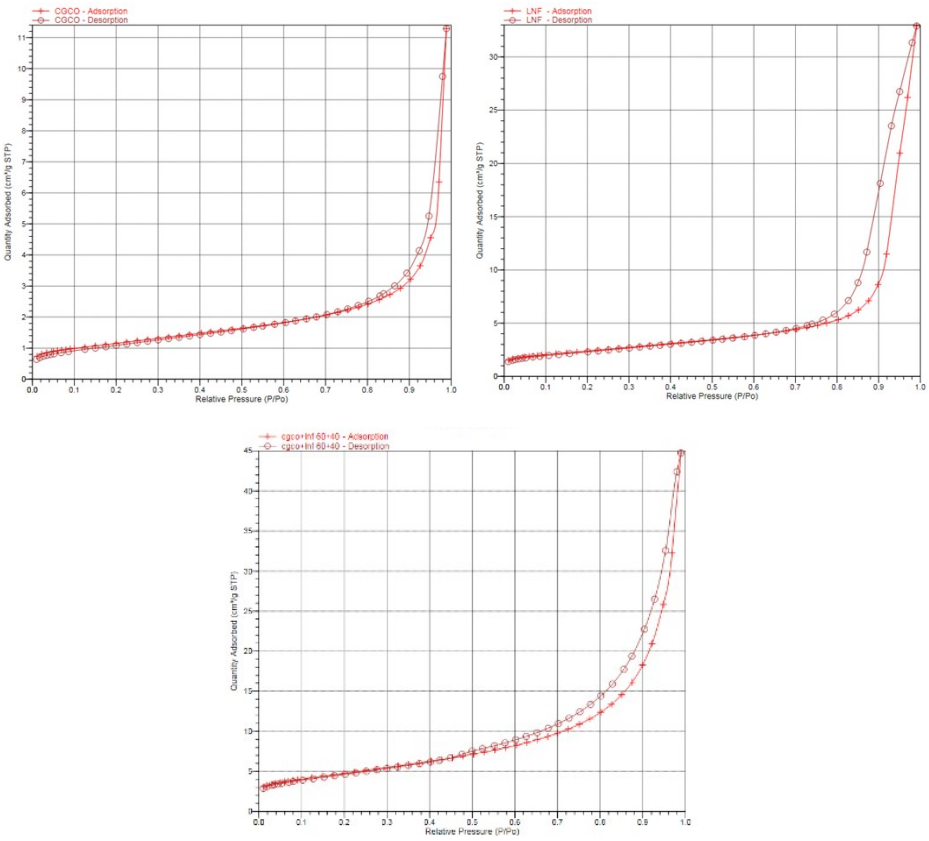

Fig. S12 N_2 adsorption/desorption isotherms of CGCO, LNF, CGCO/LNF 60/40.

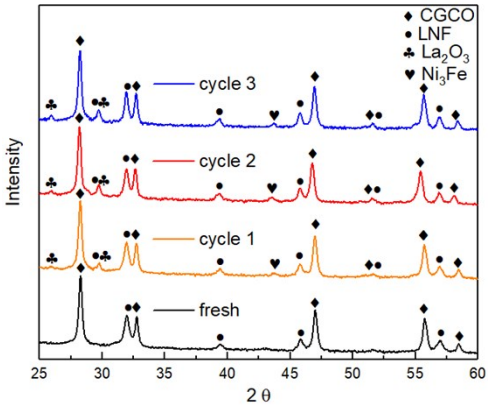

Fig. S13 *In-situ* XRD patterns of CGCO/LNF 60/40 for different redox cycles.

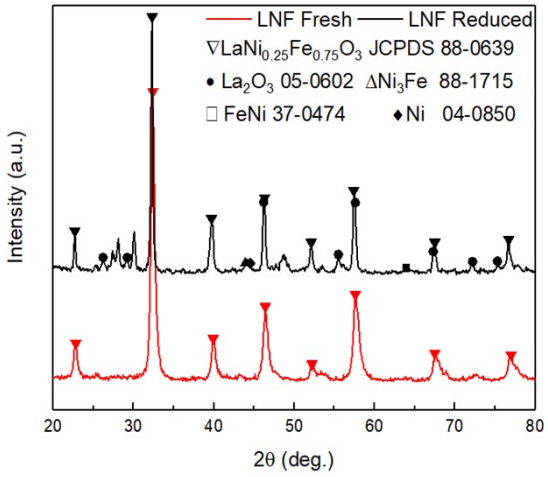

Fig. S14 XRD patterns of LNF (fresh and reduced).

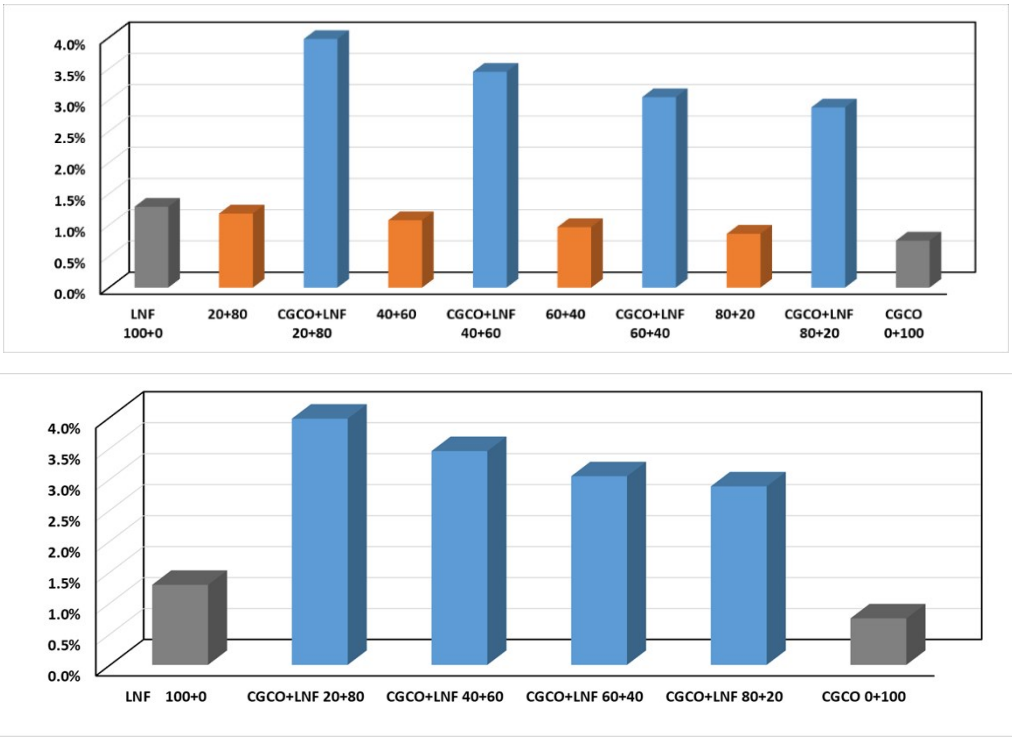

750 °C

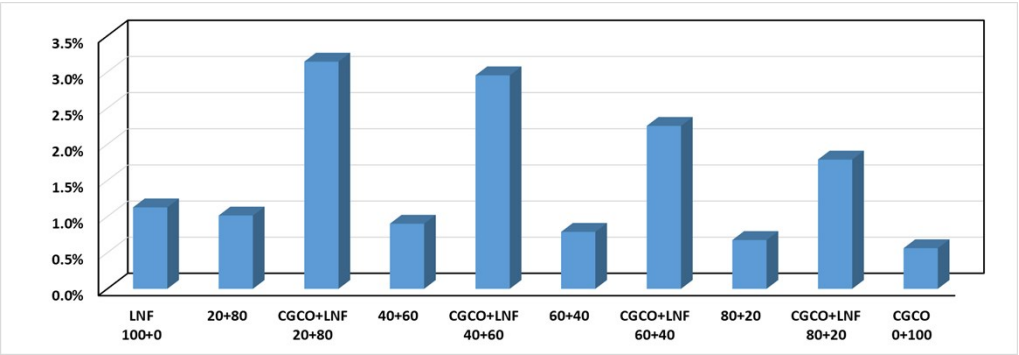

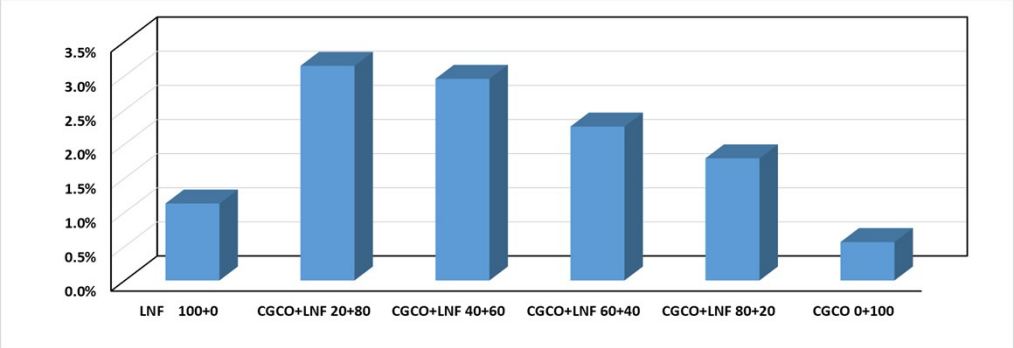
3.5%
3.0%
2.5%
2.0%
1.5%
1.0%
0.5%
0.0%
LNF 100+0
CGCO+LNF 20+80
CGCO+LNF 40+60
CGCO+LNF 60+40
CGCO+LNF 80+20
CGCO 0+100

700 °C

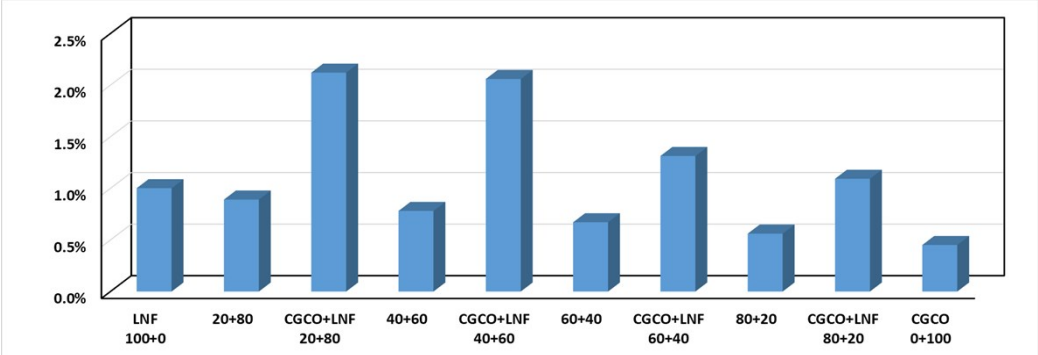
2.5%
2.0%
1.5%
1.0%
0.5%
0.0%
LNF 100+0
20+80
CGCO+LNF 20+80
40+60
CGCO+LNF 40+60
60+40
CGCO+LNF 60+40
80+20
CGCO+LNF 80+20
CGCO 0+100

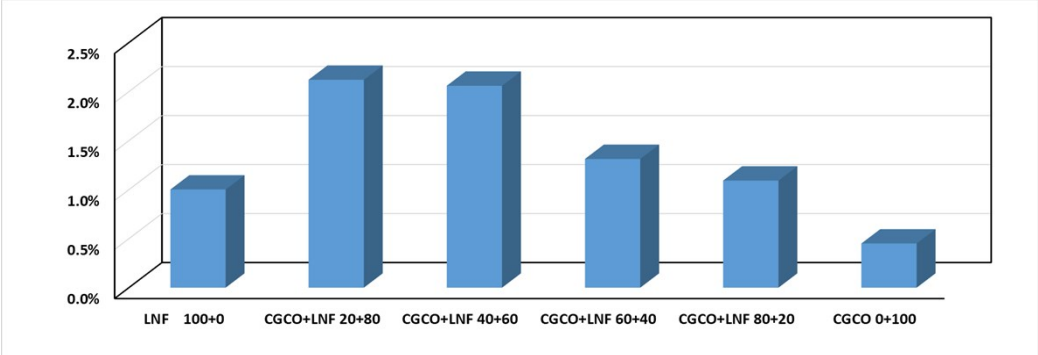
2.5%
2.0%
1.5%
1.0%
0.5%
0.0%
LNF 100+0
CGCO+LNF 20+80
CGCO+LNF 40+60
CGCO+LNF 60+40
CGCO+LNF 80+20
CGCO 0+100

650 °C

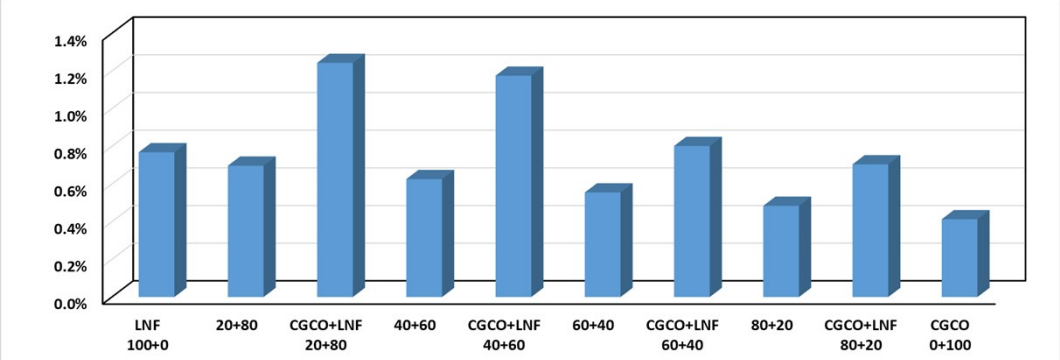
1.4%
1.2%
1.0%
0.8%
0.6%
0.4%
0.2%
0.0%
LNF 100+0
20+80
CGCO+LNF 20+80
40+60
CGCO+LNF 40+60
60+40
CGCO+LNF 60+40
80+20
CGCO+LNF 80+20
CGCO 0+100

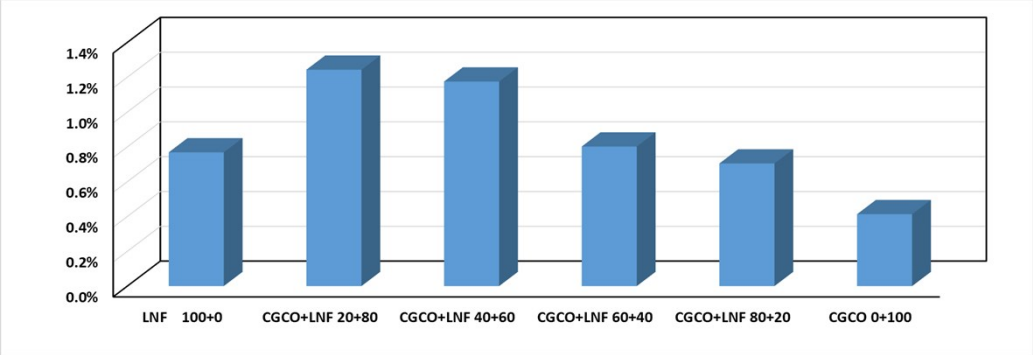

600 °C

Fig. S15 Oxygen capacity tested in the TGA reactor (750°C, 700°C, 650°C, 600°C).

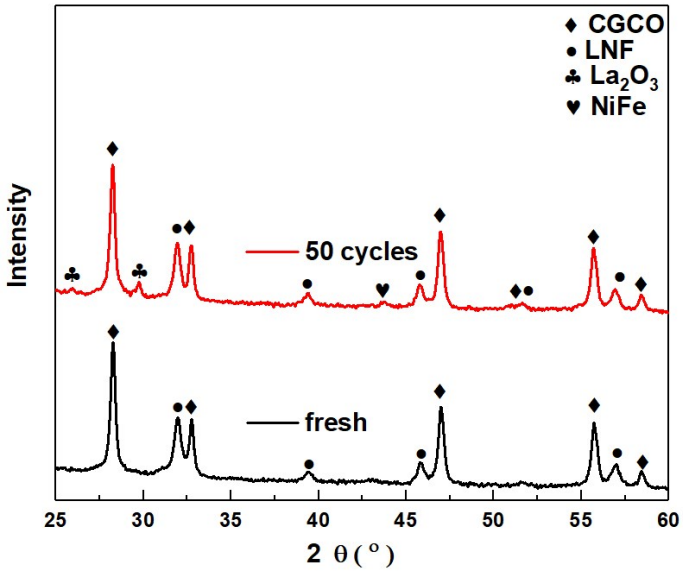

Fig. S16 XRD patterns of the fresh and cycled CGCO/LNF 60/40 after 50 redox cycles.

Table S4. Performance comparisons of the redox catalyst in this study versus the recently published redox catalysts on methane POx and CO_2 splitting

Redox catalyst composition	PGM type, content and cost ($/kg catalyst)	Optimal reaction temperature (^oC)	CO_2 conversion	Average CO_2 conv. rate (mmol kg_{cat}^{-1} s^{-1})	Methane conversion	Syngas selectivity	Average methane utilization rate (mmol kg_{cat}^{-1} s^{-1})	H_2/CO Ratio (or coking)	Ref
$LaNi_{0.35}Fe_{0.65}O_3$-$Ce_{0.85}Gd_{0.1}Cu_{0.05}O_2$	***N/A***	***750 ^oC (600 – 750 ^oC)****	***91%***	***1.36***	***91%***	***96%***	***3.79***	***2 (this study)***	
Rh-$LaCeO_{4-x}$	**0.5wt% Rh ~ $650**	**650 ^oC**	**95%**	**0.71**	**90%**	**89%**	**3.75**	**5.5% coke**	[2]
Fe/CeO_2-IMP	**N/A**	**800 ^oC**	**10%**	**1.86**	**2%**	**~2%**	**0.37**	**4.8**	
Ni/CeO_2-COM	**N/A**	**800 ^oC**	**15%**	**2.79**	**12%**	**70%**	**2.23**	**1.8**	
$CeNi_{0.3}O_y$-CP	**N/A**	**800 ^oC**	**65%**	**12.09**	**60%**	**95%**	**11.16**	**1.9**	
$CeNi_{0.5}Zr_{0.5}O_y$-CP	**N/A**	**800 ^oC**	**80%**	**14.88**	**78%**	**87%**	**14.51**	**3.5**	[3]
Co/CeO_2-IMP	**N/A**	**800 ^oC**	**80%**	**14.88**	**80%**	**90%**	**14.88**	**2**	
Ni/CeO_2-IMP	**N/A**	**800 ^oC**	**86%**	**15.9**	**88%**	**98%**	**16.3**	**~2.2 ~4% coke**	
$NiFe_2O_4$	**N/A**	**900 ^oC**	**19.86% for 1st cycle 16.38% after 3 cycles**	**7.39 for 1st cycle 6.09 after 3 cycles**	**90% 1st cycle 75% after 3 cycles**	**Not detected**	**33.48 1st cycle 27.90 after 3 cycles**	**2.5**	[4]
$Sr_3Fe_2O_{7-\delta}$-$Ca_{0.5}Mn_{0.5}O_2$	**N/A**	**900 ^oC**	**90%**	**11.96**	**95%**	**95%**	**12.62**	**1.96**	[5]
$Fe_{0.88}Ni_{0.12}O_x$ on ceria	**N/A**	**1000 ^oC**	**90%**	**6.70**	**90%**	**90%**	**5.58**	**2**	[6]
$La_{0.6}Sr_{0.4}Co_{0.2}Fe_{0.8}O_{3-\delta}$	**N/A**	**1030 ^oC**	**8%**	**3.77**	**17%**	**50%**	**1.27**	**n/a**	[7]

** the redox catalyst in this study is highly active within this temperature range.*

References Cited.

1. Vyazovkin, S.; Burnham, A. K.; Criado, J. M.; Pérez-Maqueda, L. A.; Popescu, C.; Sbirrazzuoli, N., ICTAC Kinetics Committee recommendations for performing kinetic computations on thermal analysis data. *Thermochimica Acta* **2011,** *520* (1), 1-19.
2. Haribal, V. P.; Wang, X.; Dudek, R.; Paulus, C.; Turk, B.; Gupta, R.; Li, F., Modified Ceria for "Low-Temperature" CO2 Utilization: A Chemical Looping Route to Exploit Industrial Waste Heat. *Advanced Energy Materials* **2019**, 1901963.
3. Guerrero-Caballero, J.; Kane, T.; Haidar, N.; Jalowiecki-Duhamel, L.; Lofberg, A., Ni, Co, Fe supported on Ceria and Zr doped Ceria as oxygen carriers for chemical looping dry reforming of methane. *Catalysis Today* **2019,** *333*, 251-258.
4. Huang, Z.; Jiang, H. Q.; He, F.; Chen, D. Z.; Wei, G. Q.; Zhao, K.; Zheng, A. Q.; Feng, Y. P.; Zhao, Z. L.; Li, H. B., Evaluation of multi-cycle performance of chemical looping dry reforming using CO2 as an oxidant with Fe-Ni bimetallic oxides. *Journal of Energy Chemistry* **2016,** *25* (1), 62-70.
5. Zhang, J.; Haribal, V.; Li, F., Perovskite nanocomposites as effective CO2-splitting agents in a cyclic redox scheme. *Sci Adv* **2017,** *3* (8), e1701184.
6. AmeyMore, S. B., and Gçtz Veser, Iron–Nickel Alloys for Carbon Dioxide Activation by Chemical Looping Dry Reforming of Methane. *Energy Technology* **2015,** *4*, 1147–1157.

7. Michalsky, R.; Neuhaus, D.; Steinfeld, A., Carbon Dioxide Reforming of Methane using an Isothermal Redox Membrane Reactor. *Energy Technology* **2015,** *3* (7), 784-789.